Reznychenko, M., Bogomaz, O., Kotov, D., Zhivolup, T., Koloskov, O., & Lisachenko, V. (2022). Observation of the ionosphere by ionosondes in the Southern and Northern hemispheres during geospace events in October 2021. *Ukrainian Antarctic Journal*, *20*(1), 18—30.
https://doi.org/10.33275/1727-7485.1.2022.686

M. Reznychenko [1, *], O. Bogomaz [1, 2], D. Kotov [1], T. Zhivolup [1], O. Koloskov [3, 2], V. Lisachenko [3]

[1] Institute of Ionosphere, National Academy of Sciences of Ukraine, Ministry of Education and Science of Ukraine, Kharkiv, 61001, Ukraine
[2] State Institution National Antarctic Scientific Center, Ministry of Education and Science of Ukraine, Kyiv, 01601, Ukraine
[3] Institute of Radio Astronomy, National Academy of Sciences of Ukraine, Kharkiv, 61002, Ukraine

*** Corresponding author:** marina.shulga23@gmail.com

Observation of the ionosphere by ionosondes in the Southern and Northern hemispheres during geospace events in October 2021

Abstract. The paper presents the results of ionospheric observations performed over the Ukrainian Antarctic Akademik Vernadsky station and Millstone Hill (USA). Ionospheric parameters such as peak electron density and height ($h_{m\mathrm{F2}}$ and $N_{m\mathrm{F2}}$) in October 2021 are shown and discussed. The results of the comparative analysis between observations and predictions of the International Reference Ionosphere 2016 (IRI-2016) model are presented. The main objectives of this work are an investigation of the ionosphere response to space weather effects in the Northern and Southern hemispheres in the American longitudinal sector using ionosondes located at the Vernadsky station and near the magnetically conjugate region – Millstone Hill, and a comparison of observations with the model. The F2-layer peak height was calculated from ionograms obtained by ionosonde using subsequent electron density profile inversion. Diurnal variations of $h_{m\mathrm{F2}}$ and $N_{m\mathrm{F2}}$ were calculated using a set of sub-models of the IRI-2016 model for comparison with experimental results. A strong negative response of the ionosphere to the moderate geomagnetic storm on October 12, 2021 was revealed over the Vernadsky station and Millstone Hill. During October 21–31, 2021, the gradual night-to-night increase in $N_{m\mathrm{F2}}$ (by a factor of ~2) was observed over the Vernadsky station. It was found that the IRI $h_{m\mathrm{F2}}$ sub-models (SHU-2015 and AMTB-2013) provide a relatively good agreement with the observed variations of $h_{m\mathrm{F2}}$ in the daytime and nighttime for almost the entire investigated period over both the Vernadsky station and Millstone Hill. The largest deviations for both IRI $h_{m\mathrm{F2}}$ sub-models occurred during the nighttime of geomagnetically disturbed periods. The IRI $N_{m\mathrm{F2}}$ sub-models (URSI and CCIR) generally agree with the observations. However, observations and model predictions differ somewhat in the geomagnetically disturbed periods. According to the results of the standard deviation calculations, it cannot be concluded that any of the IRI-2016 sub-models is better than the others. The hypotheses on the possible reasons for the differences in the modeled and observed variations of $h_{m\mathrm{F2}}$ and $N_{m\mathrm{F2}}$ are proposed and discussed in the frame of well-known ionospheric storms' mechanisms. The results obtained in this paper demonstrate the peculiarities of the ionosphere in different hemispheres of the American longitude sector under geomagnetically quiet and disturbed conditions and provide one more validation of the modern empirical international reference models of the ionosphere.

Keywords: electron density, F2-layer peak height, geomagnetic storm, ionospheric model, ionospheric vertical sounding

1 Introduction

The vertical sounding of the ionosphere (VSI) is an indispensable remote sensing technique that provides operative information about the ionosphere and its coupling with the upper atmosphere. The vertical sounding is carried out by means of ionosondes – high-frequency (HF) pulsed radars designed to obtain altitude profiles of the electron density up to the F2-layer peak height. The relatively low cost of the equipment, low power consumption, and continuous operation are key advantages of the ionosonde for ionospheric study (Reinisch et al., 2009).

The ionospheric study has been provided at the Ukrainian Antarctic Akademik Vernadsky station (hereinafter – Vernadsky station) for many years using ionosonde, which is one of the few instruments for geospace research at high geographic latitudes of the Southern hemisphere (Zalizovskiy et al., 2018; Koloskov et al., 2019). Location of the ionosonde at Vernadsky station is 65.25°S, 295.75°E, with L ≈ 2.74 as calculated at the height of h = 250 km in 2021 from https://ccmc.gsfc.nasa.gov/modelweb/models/igrf_vitmo.php. The ionosonde at Millstone Hill (MH) (42.6°N, 288.5°E, L ≈ 2.64) is located in the region that is close to the Northern end of the magnetic flux tube passing over the Vernadsky station. That allows studying the reaction of the ionosphere to space weather effects simultaneously for the magnetically conjugated points in the Northern and Southern hemispheres in the American longitudinal sector.

Shulha et al. (2019) conducted multi-instrumental studies of the ionospheric response to a weak geomagnetic storm in the American longitudinal sector during the equinox on March 21–23, 2017. For our study, the period of October, 2021 was selected because this is a transition period to the summer/winter solstice conditions, which occur in the Southern/Northern hemispheres in December. Moreover, given the location of the Vernadsky station, this period is interesting to study manifestations of seasonal variations of the Weddell Sea Anomaly (Bellchambers & Piggott, 1958; Dudeney & Piggott, 1978).

2 Data and methods

Information about the state of the ionosphere at the Vernadsky station was obtained by a digital ionosonde designed jointly by the Institute of Radio Astronomy of National Academy of Sciences of Ukraine and the Abdus Salam International Centre for Theoretical Physics (Koloskov et al., 2019). It is based on the software-defined radio concept that provides good system flexibility. The ionosonde consists of the USRP N200 kit, ZX80-DR230+ antenna switch, ICOM IC-718 transceiver (used as the 100 W power amplifier), SP-200-13.5 power supply unit, and a personal computer.

The ionosonde operating mode parameters are listed in Table 1.

Critical frequencies and traces of F2, F1, and E layers obtained by the ionosonde installed at the Vernadsky station were manually scaled for electron density profile inversion using NHPC program version 4.30 (Huang & Reinisch, 1996). Ionograms were scaled using the IonogramViewer2 software. The validity of such a technique was proven by a number of investigations (Bogomaz et al., 2019a; 2019b; Shulha et al., 2019). The F2-layer peak electron density $N_{m\mathrm{F2}}$ was calculated from the critical frequency of F2-layer f_{oF2} using the relation $N_{m\mathrm{F2}} = 1.24 \cdot 10^{10} f_{\mathrm{oF2}}{}^2$), where f_{oF2} is expressed in MHz.

Ionospheric characteristics at MH were obtained by the digisonde DPS-4D. This digisonde is a part of the Global Ionospheric Radio Observatory (GIRO) (Reinisch & Galkin, 2011). The digisonde operating mode parameters in October 2021 are listed in Table 2.

Table 1. Operating mode parameters of the ionosonde at the Vernadsky station, October 2021

Parameter	Value
Frequency range	1–16 MHz
Number of frequencies	320
Virtual height range	90–800 km
Total heights (related to the sampling rate of 200 kS/s)	942
Transmitter pulse width (16 code chips)	600 μs (16 × 37.5 μs)

Table 2. Operating mode parameters of the digisonde at Millstone Hill

Parameter	Value
Frequency range	1—10 MHz
Number of frequencies	360
Virtual height range	80—1360 km
Total heights	512

Ionograms obtained by the MH digisonde were processed using the SAO Explorer program version 3.6.1. It contains the Automatic Real Time Ionogram Scaler with True height (ARTIST) software (Galkin et al., 2008) and the NHPC program version 4.34. All the results of ionogram scaling by the ARTIST software were additionally verified and edited manually before applying the electron density profile inversion. At the time of writing this paper, the GIRO database contained data only for October 6 to 29. The International Reference Ionosphere model (IRI-2016) was used to compare the observed ionospheric parameters $h_{m\mathrm{F2}}$ and $N_{m\mathrm{F2}}$ with the model predictions. An overview and information about the latest modifications of this model are presented in (Bilitza et al., 2017).

Electron F2-layer peak density $N_{m\mathrm{F2}}$ and electron F2-layer peak height $h_{m\mathrm{F2}}$ were obtained using sub-models implemented in IRI-2016. The Comité Consultatif International pour la Radio (CCIR) (International Radio Consultative Committee, 1967) and Union Radio Scientifique Internationale (URSI) (Rush et al., 1989) sub-models were used to obtain $N_{m\mathrm{F2}}$. Both $N_{m\mathrm{F2}}$ sub-models are governed by the solar activity indices and have the "F-peak storm model" option (Fuller-Rowell et al., 1998; 2000) aimed to reflect an average storm behavior in $N_{m\mathrm{F2}}$ based on the a_p history over the preceding 33 hours. The SHU-2015 (Shubin, 2015) and AMTB-2013 (Altadill et al., 2013) sub-models were used to obtain $h_{m\mathrm{F2}}$. Both $h_{m\mathrm{F2}}$ sub-models are also governed by solar activity indices, but they are insensitive to changes of the magnetic activity.

3 Results and discussion

For a study of the space weather influence on the ionosphere in the Northern and Southern hemispheres in the American longitudinal sector, the period of October 1—31, 2021, UTC time, was selected (Fig. 1). The solar activity level during October 1–22 was low and stable ($F_{10.7}$ solar radio flux index did not exceed 90 sfu), while the period of October 23—31 was characterized by moderate solar activity ($F_{10.7} > 100$ sfu). The geomagnetic conditions were relatively quiet (the planetary index of geomagnetic activity K_p did not exceed 4), except for October 12, 2021, when K_p reached 6. At the same time, significant changes in variations of solar wind parameters were observed. Due to the effect of the M1.6 solar flare event and the Coronal Mass Ejection (CME) on October 9, 2021 (https://blogs.nasa.gov/solarcycle25/2021/10/), the solar wind velocity (V_{SW}) sharply increased from 400 to 500 km/s on October 12, 2021. These intervals of V_{SW} increase are notable for enhancements in solar wind proton density (N_{SW}) and increase in the amplitude of the interplanetary magnetic field (IMF) B_z component ($-6 < B_z < 6$ nT). The minimum SYM/H geomagnetic index was –60 nT, indicating a moderate geomagnetic storm (Gonzalez et al., 1994; Shinbori et al., 2022).

The diurnal variations of the ionospheric parameters $h_{m\mathrm{F2}}$ and $N_{m\mathrm{F2}}$ over the Vernadsky station and MH are shown in Figures 2 and 3. It is seen that $h_{m\mathrm{F2}}$ variations over the Vernadsky station and MH represent the quiet conditions. Over the Vernadsky station, for the entire investigated period, the minimum value of $h_{m\mathrm{F2}}$ during the daytime was ~230 km, except for October 10—11 and 28—31, when an increase in $h_{m\mathrm{F2}}$ by ~20 km was observed. During the nighttime, the minimum value of $h_{m\mathrm{F2}}$ was ~360 km. A comparison of $h_{m\mathrm{F2}}$ variations for the Vernadsky station and MH revealed some differences. During the entire study period, the nighttime $h_{m\mathrm{F2}}$ values over Millstone Hill were ~15% lower than over the Vernadsky station. During the daytime, variations in $h_{m\mathrm{F2}}$ over the Vernadsky station and MH were almost indistinguishable. These results indicate that during nighttime in the middle latitudes of the Northern hemisphere, the ionosphere was lower than in the Southern hemisphere over the Vernadsky station.

Comparing the state of the ionosphere over the Vernadsky station and Millstone Hill, the daytime decrease of the critical frequency ($f_{o\mathrm{F2}}$) was observed on

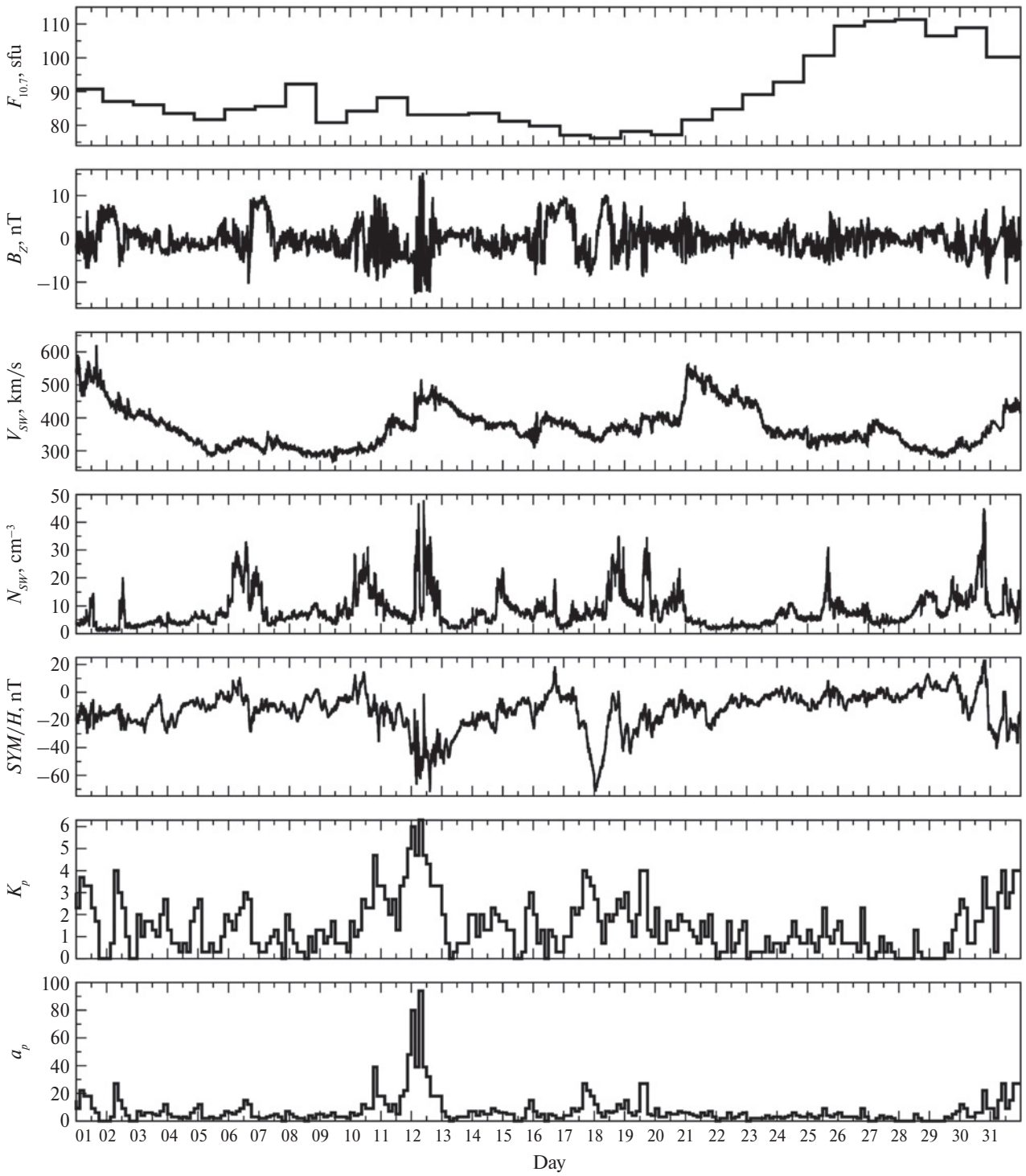

Figure 1. Variations of the parameters describing space weather during October 01—31, 2021 (from top to bottom): daily solar activity $F_{10.7}$ index, the north-south (B_z) component of the interplanetary magnetic field (IMF), solar wind velocity (V_{SW}), solar wind proton density (N_{SW}), *SYM/H* index, 3-hour K_p index and 3-hour a_p index

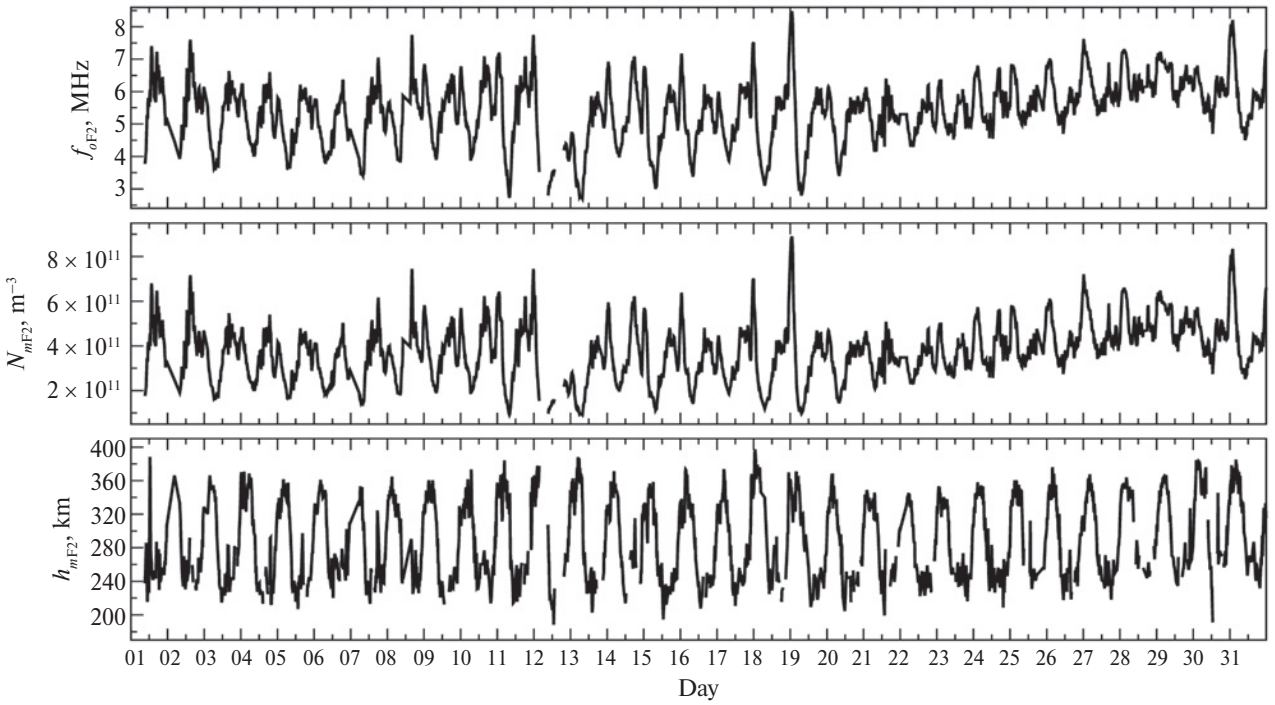

Figure 2. The critical frequency of the F2 layer f_{oF2} obtained by scaling ionograms of ionosonde at the Vernadsky station (top), calculated electron F2-layer peak density N_{mF2} (middle), and the evaluated electron F2-layer peak height h_{mF2} (bottom). October, 2021

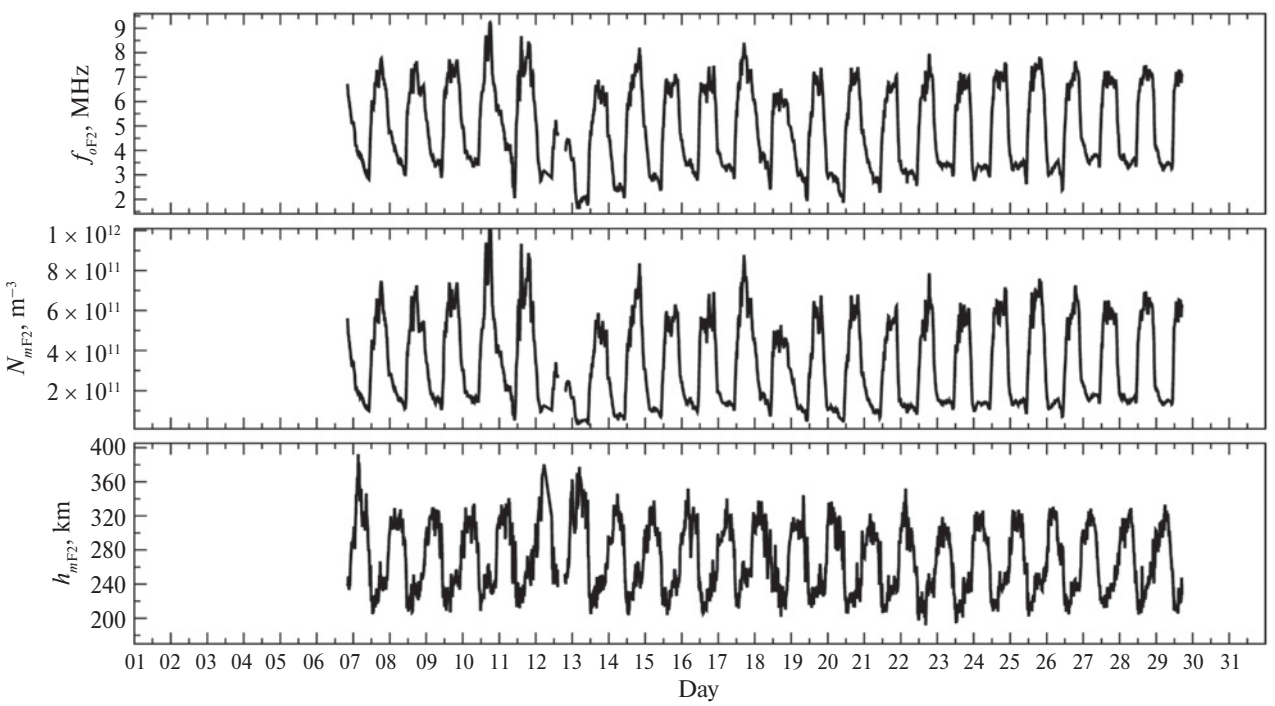

Figure 3. The critical frequency of the F2 layer f_{oF2} obtained by scaling ionograms of ionosonde located at MH (top), calculated electron F2-layer peak density N_{mF2} (middle) and evaluated electron F2-layer peak height h_{mF2} (bottom). October, 2021

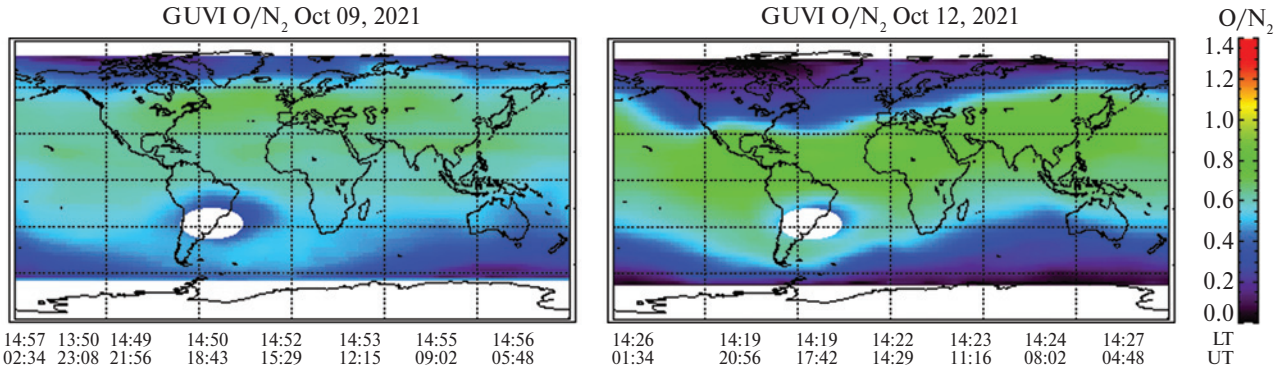

Figure 4. The thermospheric O/N_2 ratio obtained from the TIMED/GUVI instrument for a quiet day of October 9, 2021 (left panel) and a stormy day of October 12, 2021 (right panel) (http://guvitimed.jhuapl.edu/guvi-galleryl3on2)

October 12, 2021. At the same time, N_{mF2} decreased almost three-fold compared to the preceding days of quiet magnetic conditions, indicating the presence of the negative ionospheric storm. Such significant daytime decreases of N_{mF2} were likely caused by a strong heating of the neutral atmosphere and, consequently, an increase in the molecular nitrogen density (N_2), which is responsible for the recombination of plasma in the ionosphere (Rees & Fuller-Rowell, 1992; Rishbeth, 1998). The thermospheric O/N_2 ratio obtained from the TIMED/GUVI instrument for geomagnetically quiet (October 9, 2021) and disturbed (October 12, 2021) days is shown in Figure 4; a decrease in the O/N_2 ratio occurred during the storm-time period in the high latitudes of the Southern hemisphere near the Vernadsky station and the mid-latitudes of the Northern hemispheres near MH.

Unfortunately, due to the lack of observational data on h_{mF2} during the daytime on October 12, it is difficult to make reliable conclusions about the effect of changes in plasma transport (variations of thermospheric winds or magnetosphere electric field) on N_{mF2}.

The nighttime N_{mF2} values during October 11—12 and 12—13 also decreased almost twice compared to the previous nights over Vernadsky station and MH. The probable reason for such a decrease in N_{mF2} is the heating of the neutral atmosphere too. Another probable reason is the partial depletion of the plasmaspheric flux tube and, consequently, the decrease of nighttime plasma fluxes into the ionosphere, which, in turn, led to a decrease in N_{mF2} (Richards et al., 1983; 2000). A similar result of the N_{mF2} response to a moderate geomagnetic storm was described in (Kotov et al., 2018).

The October 21—31, 2021 period deserves special consideration. Starting from October 21, the gradual night-to-night increase in F2-layer peak density was observed over the Vernadsky station, which peaked between October 28 and 29. The nighttime N_{mF2} increased ~2 times and was almost equal to the daytime N_{mF2} values. It should be noted that such an increase in N_{mF2} followed the enhancement in $F_{10.7}$ index values (Fig. 1). Such an increase of N_{mF2} over MH was not observed. The probable reason for the N_{mF2} enhancement above the Vernadsky station during the nighttime is that October is the period of transition to the summer solstice conditions in the Southern hemisphere when the Weddell Sea anomaly is pronounced over the Antarctic Peninsula (Dudeney & Piggott, 1978; Horvath & Essex, 2003). The observed decrease in the difference between daytime and nighttime N_{mF2} values can indicate gradual development of this anomaly.

Figures 5 and 6 show the diurnal variations of the ionospheric parameters h_{mF2} and N_{mF2} calculated using the IRI-2016 model for the Vernadsky station and MH. Generally, the IRI N_{mF2} sub-models reproduce the negative ionospheric storm on October 12, 2021 well. At the same time, the sub-models predict a decrease in N_{mF2} by ~20 % for the Vernadsky station and MH. It should also be noted that URSI and CCIR sub-models are a good fit for the changes in night-

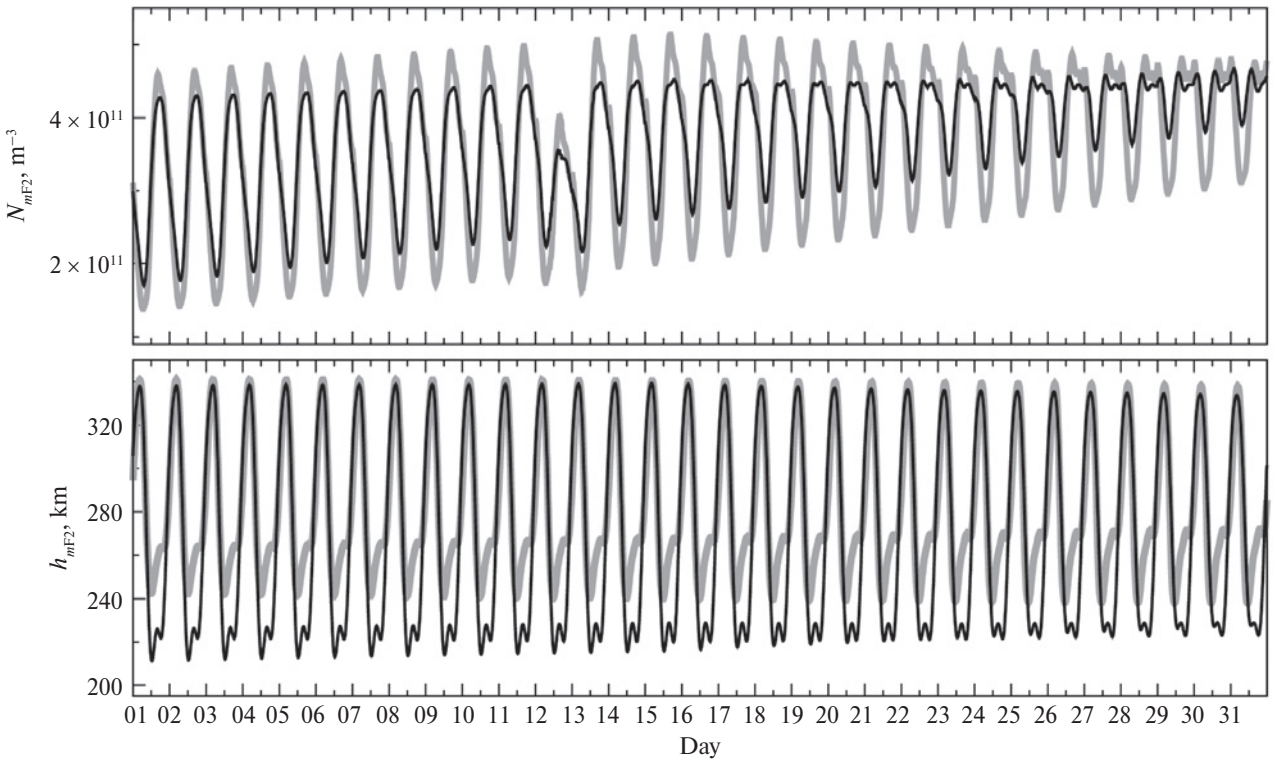

Figure 5. N_{mF2} and h_{mF2} simulations for the Vernadsky station, October 01—31, 2021. Black lines: URSI and SHU-2015, gray lines: CCIR and AMTB-2013

time variations of N_{mF2} during the October 21—31, 2021 period over the Vernadsky station.

The IRI h_{mF2} sub-models show a realistic average and typical behavior for the Vernadsky station and MH. There is good agreement between the SHU-2015 and AMTB-2013 models during nighttime for the Vernadsky station and during daytime for Millstone Hill.

The diurnal variations of ionospheric parameters h_{mF2} and N_{mF2} obtained using IRI-2016 model calculations and observational data of ionosondes located at the Vernadsky station and MH are shown in Figures 7 and 8. The standard deviations (SD) of the difference between experimental and modeled data for the h_{mF2} and N_{mF2} sub-models were calculated (Table 3).

Table 3. Standard deviations of the experimental and modeled data differences for different IRI-2016 options

IRI-2016 sub-model	SD for the Vernadsky station	SD for Millstone Hill
SHU-2015	24.92 km	18.98 km
AMTB-2013	27.93 km	23.13 km
URSI	$1.14 \cdot 10^{11}$ m^{-3}	$1.04 \cdot 10^{11}$ m^{-3}
CCIR	$1.02 \cdot 10^{11}$ m^{-3}	$1.06 \cdot 10^{11}$ m^{-3}

The SHU-2015 model shows a good agreement with the observed variations of h_{mF2} for almost the entire investigated period, both during the daytime and nighttime. The largest deviations are observed during the nighttime of the geomagnetically disturbed period (October 12—13), when the SHU-2015 model underestimates the nighttime value of h_{mF2} (by ~40 km) over both the Vernadsky station and MH and during the nighttime of October 17—18 over the Vernadsky station.

The F2-layer peak height obtained using the AMTB-2013 sub-model is much closer to the observed values during the nighttime of October 12 and 13 at mid-latitudes over MH. However, over the Vernadsky station, the sub-model overestimates the values of F2-

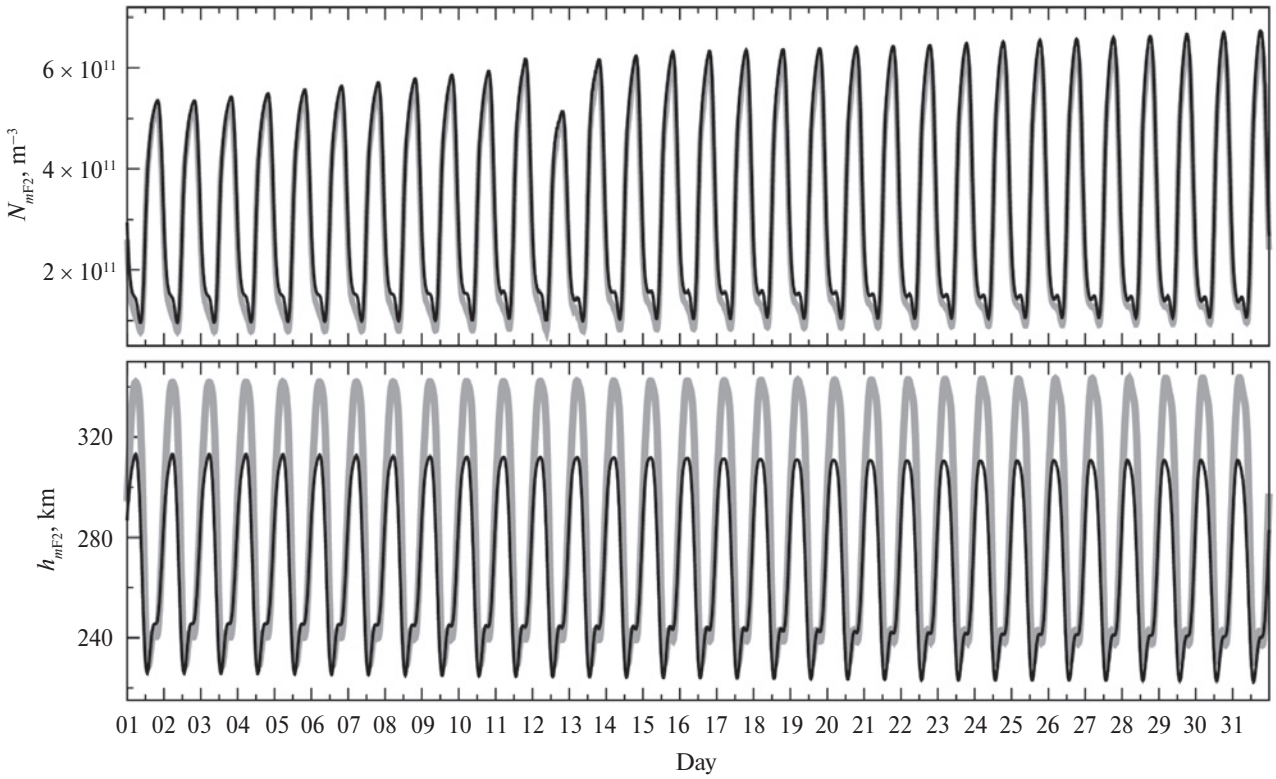

Figure 6. N_{mF2} and h_{mF2} simulations for MH. Black lines: URSI and SHU-2015, gray lines: CCIR and AMTB-2013

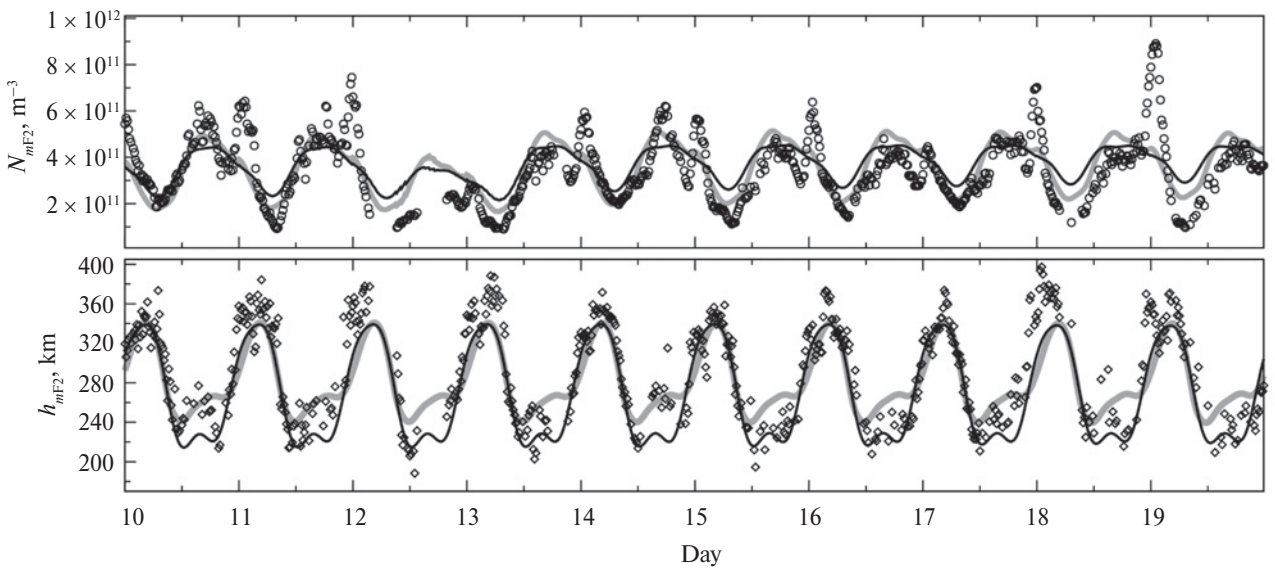

Figure 7. Comparison of the experimental results obtained for the Vernadsky station (circles and rhombs) with model values (lines) during October 10—19, 2021. Black lines: URSI and SHU-2015, gray lines: CCIR and AMTB-2013

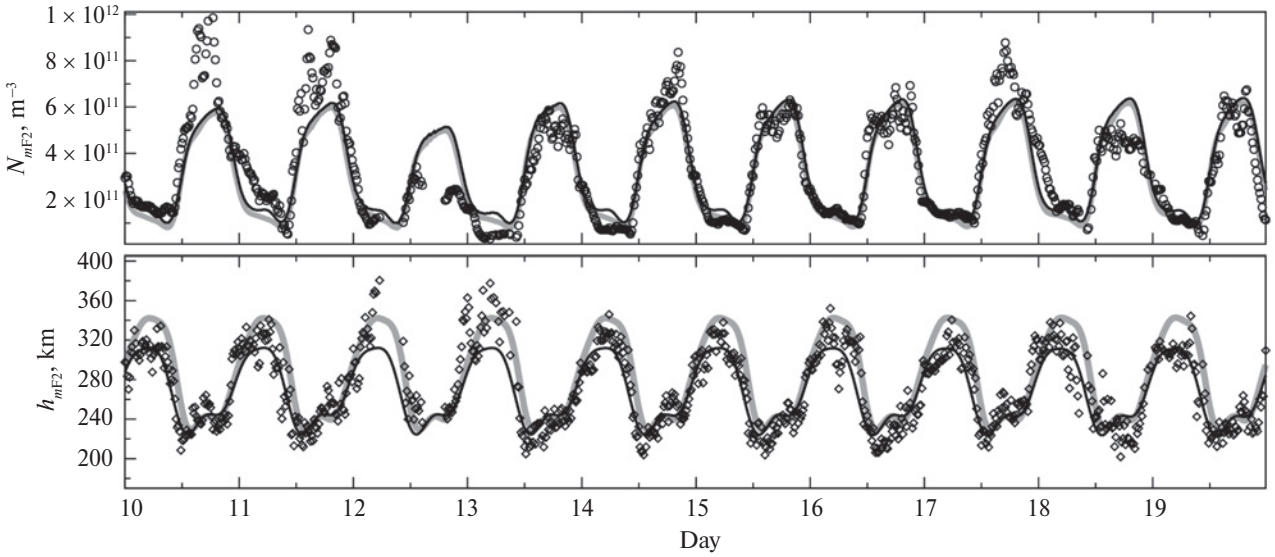

Figure 8. Comparison of the experimental results obtained for MH (circles and rhombs) with model values (lines) during October 10–19, 2021. Black lines: URSI and SHU-2015, gray lines: CCIR and AMTB-2013

layer peak height during the daytime (by ~20 km) and significantly underestimates (by ~40 km) the h_{mF2} values during the nighttime on October 12, 13, and 18, 2021. The obtained results demonstrate that the ionospheric layers over the Vernadsky station are located higher during the nighttime of geomagnetically disturbed periods compared to the AMTB-2013 model predictions.

Based on the SD calculations for the h_{mF2} sub-models, it cannot be concluded that any sub-model is preferable to use (Table 3).

The IRI N_{mF2} sub-models (URSI and CCIR) generally agree with the observations for the Vernadsky station and MH. However, some discrepancies between observations and model predictions are observed during the daytime on October 10, 11, and 17, 2021 over MH, when the N_{mF2} models underestimate the experimental values by a factor of ~1.5. Both IRI N_{mF2} models overestimate the N_{mF2} values during the nighttime for a geomagnetically disturbed period of October 12—13, 2021 by a factor of ~2. The probable reason for the difference between the observed and model results on October 12, 2021 is that the IRI N_{mF2} sub-models do not reproduce the real processes with a probable heating of the neutral atmosphere or partial depletion of the magnetic flux tube. Due to the lack of experimental f_{oF2} and N_{mF2} data, it is impossible to make reliable conclusions about the differences between the observed and modeled data during the daytime of October 12, 2021. Similar to the case of the h_{mF2} sub-models results, it cannot be concluded that some of the N_{mF2} sub-models are preferable for the period under consideration (Table 3).

4 Conclusions

The main results are the following:

1. Diurnal variations in the ionospheric parameters h_{mF2} and N_{mF2} obtained from ionosondes in the Northern and Southern hemispheres in the American longitudinal sector for October 2021 were analyzed.

2. A strong negative response of the ionosphere to a moderate geomagnetic storm on October 12, 2021 was revealed over the Vernadsky station and MH. There is a three-fold decrease in the F2-layer peak density N_{mF2} during the daytime of the disturbed period. The probable reason for this decrease in N_{mF2} is the heating of the neutral atmosphere in the auroral regions. TIMED/GUVI observations of the O/N_2 ratio support this hypothesis. A two-fold decrease in N_{mF2} values during the nighttime of the disturbed period may

be caused by the partial depletion of the plasmaspheric flux tube.

3. During October 21—31, 2021 the gradual night-to-night increase in N_{mF2} was observed over the Vernadsky station. At the same time, the N_{mF2} values increased by a factor of ~2. The probable reason for this N_{mF2} enhancement is that October is a transitional period to the summer solstice conditions in the Southern hemisphere when the Weddell Sea Anomaly is pronounced over the Antarctic Peninsula.

4. The observations were compared to the IRI-2016 model predictions. The SHU-2015 sub-model showed a good agreement with the observed variations of h_{mF2} for almost the entire investigated period, both during the daytime and nighttime. The largest deviations were observed during the nighttime of geomagnetically disturbed periods. The AMTB-2013 model agrees well with the observed results for MH during the nighttime of October 12 and 13, 2021. However, there are some discrepancies for the Vernadsky station, where the model overestimates the F2-layer peak height values during the daytime (by ~20 km) and underestimates (by ~40 km) the h_{mF2} values during the nighttime of geomagnetically disturbed periods. According to SD calculations for the h_{mF2} sub-models any of the sub-models is not preferable to use for the investigated period.

5. The IRI N_{mF2} sub-models (URSI and CCIR) generally agree with the observations. However, the predictions differ from the data for geomagnetically disturbed periods. Both IRI N_{mF2} sub-models overestimate N_{mF2} values during the nighttime for a geomagnetically disturbed period of October 12, 2021 by a factor of ~2. The probable reason for such a difference between the observed and modeled results is that the IRI N_{mF2} sub-models do not reproduce the real picture with probable heating of the neutral atmosphere or partial depletion of the magnetic flux tube. As in the case of the h_{mF2} sub-models, it cannot be concluded that any of the N_{mF2} sub-models is better to use for the period under consideration.

6. Overall conclusion is that N_{mF2} and h_{mF2} sub-models of IRI still cannot reproduce variations over American sub-auroral regions with acceptable accuracy. Despite this, the N_{mF2} sub-models qualitatively reflect key features of the variations during the quiet and disturbed periods. This is less valid for h_{mF2} sub-models, which are utterly insensitive to changes in magnetic activity.

Data and software. The IonogramViewer2 program can be downloaded from the repository on GitHub (retrieved February 3, 2022, https://github.com/Albom/IonogramViewer2). The NHPC program can be downloaded from the UMass Lowell Space Science Lab website (retrieved February 3, 2022, https://ulcar.uml.edu/SoftwareUtilities/NHPC/NHPC430.ZIP). Space weather indices were taken from the OMNIWeb (retrieved February 6, 2022, https://omniweb.gsfc.nasa.gov/form/omni_min.html). International Reference Ionosphere (2016) online version is available on the Community Coordinated Modeling Center website (retrieved April 30, 2022, https://ccmc.gsfc.nasa.gov/modelweb/models/iri2016_vitmo.php). Sunspot number file used in the Ionogram Viewer 2 program is provided by the Solar Influences Data Analysis Center (a part of the Royal Observatory of Belgium) and are available on the SIDC website (retrieved February 4, 2022, http://www.sidc.be/silso/DATA/SN_d_tot_V2.0.txt). The authors thank the University of Massachusetts at Lowell for making available the GIRO data resources (retrieved February 4, 2022, http://spase.info/SMWG/Observatory/GIRO) and the SAO Explorer program (retrieved February 4, 2022, http://ulcar.uml.edu/SAO-X/SAO-X.html). The authors acknowledge the Global Ultraviolet Imager (GUVI) for the thermospheric O/N_2 ratio data (retrieved May 1, 2022, http://guvitimed.jhuapl.edu/index.php/guvigalleryl3on2).

Author contributions. The idea, data processing, and illustration preparing: OB. Data acquisition and preparation: OK and VL. Simulations: MR. Interpretation of the results: DK and MR. Writing: OB, MR, DK, and TZ. Manuscript review and editing: MR, DK, and OK.

Funding. The study was done in the framework of the State Special-Purpose Research Program in Antarctica for 2011—2023 (Grant #0120U104549), financed by the State Institution National Antarctic

Scientific Center of the Ministry of Education and Science of Ukraine in 2021.

Acknowledgments. The authors are sincerely grateful to all defenders of Ukraine for the opportunity to prepare this article.

Conflict of Interest. The authors declare no conflict of interests.

References

Altadill, D., Magdaleno, S., Torta, J. M., & Blanch, E. (2013). Global empirical models of the density peak height and of the equivalent scale height for quiet conditions. *Advances in Space Research, 52*(10), 1756–1769. https://www.doi.org/10.1016/j.asr.2012.11.018

Bellchambers, W. H., & Piggott, W. R. (1958). Ionospheric measurements made at Halley Bay. *Nature*, 182, 1596–1597. https://doi.org/10.1038/1821596a0

Bilitza, D., Altadill, D., Truhlik, V., Shubin, V., Galkin, I., Reinisch, B., & Huang, X. (2017). International Reference Ionosphere 2016: From ionospheric climate to real-time weather predictions. *Space Weather*, *15*(2), 418–429. https://doi.org/10.1002/2016SW001593

Bogomaz, O. V., Kotov, D. V., Shulha, M. O., & Gorobets, M. V. (2019a). Comparison of the F2-layer peak height variations obtained by ionosonde and incoherent scatter radar. *Bulletin of the National Technical University "KhPI". Series: Radiophysics and ionosphere*, *25*(1350), 58–61. Retrieved March 10, 2022, from http://iion.org.ua/article/bulletin-25/

Bogomaz, O. V., Shulha, M. O., Kotov, D. V., Zhivolup, T. G., Koloskov, A. V., Zalizovski, A. V., Kashcheyev, S. B., Reznychenko, A. I., Hairston, M. R., & Truhlik, V. (2019b). Ionosphere over Ukrainian Antarctic Akademik Vernadsky station under minima of solar and magnetic activities, and daily insolation: case study for June 2019. *Ukrainian Antarctic Journal*, 19, 84—93. https://doi.org/10.33275/1727-7485.2(19).2019.154

Dudeney, J. R., & Piggott, W. R. (1978). Antarctic ionospheric research. *Antarctic Research Series*, 29, 200–235.

Fuller-Rowell, T. J., Codrescu, M. V., Araujo-Pradere, E., & Kutiev, I. (1998). Progress in developing a storm-time ionospheric correction model. *Advances in Space Research*, *22*(6), 821–827. https://doi.org/10.1016/S0273-1177(98)00105-7

Fuller-Rowell, T. J., Araujo-Pradere, E., & Codrescu, M. V. (2000). An empirical ionospheric storm-time correction model. *Advances in Space Research*, *25*(1), 139–146. https://doi.org/10.1016/S0273-1177(99)00911-4

Galkin, I. A., Khmyrov, G. M., Kozlov, A. V., Reinisch, B. W., Huang, X., & Paznukhov, V. V. (2008). The ARTIST 5. *AIP Conference Proceedings*, *974*(1), 150–159. https://doi.org/10.1063/1.2885024

Gonzalez, W. D., Joselyn, J. A., Kamide, Y., Kroehl, H. W., Rostoker, G., Tsurutani, B. T., & Vasyliunas, V. M. (1994). What is a geomagnetic storm? *Journal of Geophysical Research: Space Physics, 99*(A4), 5771—5792. https://doi.org/10.1029/93JA02867

Horvath, I., & Essex, E. A. (2003). The Weddell sea anomaly observed with the TOPEX satellite data. *Journal of Atmospheric and Solar-Terrestrial Physics*, *65*(6), 693–706. https://doi.org/10.1016/S1364-6826(03)00083-X

Huang, X., & Reinisch, B. W. (1996). Vertical electron density profiles from the Digisonde network. *Advances in Space Research*, *18*(6), 121–129. https://doi.org/10.1016/0273-1177(95)00912-4

International Radio Consultative Committee (CCIR). (1967). Atlas of ionospheric characteristics. (Report No. 340). *International Telecommunication Union*.

Koloskov, O. V., Kashcheyev, A. S., Zalizovski, A. V., Kashcheyev, S. B., Budanov, O. V., Charkina, O. V., Pikulik, I. I., Lysachenko, V. M., Sopin, A. O., & Reznychenko, A. I. (2019). New digital ionosonde developed for Vernadsky Station. In *Book of Abstracts "IX International Antarctic Conference dedicated to the 60th anniversary of the signing of the Antarctic Treaty in the name of peace and development of international cooperation"* (pp. 170–171). SI NASC. http://uac.gov.ua/international-cooperation/mak/mak-2019/

Kotov, D. V., Richards, P. G., Truhlík, V., Bogomaz, O. V., Shulha, M. O., Maruyama, N., Hairston, M., Miyoshi, Y., Kasahara, Y., Kumamoto, A., Tsuchiya, F., Matsuoka, A., Shinohara, I., Hernández-Pajares, M., Domnin, I. F., Zhivolup, T. G., Emelyanov, L. Ya., & Chepurnyy, Ya. M. (2018). Coincident observations by the Kharkiv IS radar and ionosonde, DMSP and Arase (ERG) satellites, and FLIP model simulations: Implications for the NRLMSISE-00 hydrogen density, plasmasphere, and ionosphere. *Geophysical Research Letters*, *45*(16), 8062–8071. https://doi.org/10.1029/2018GL079206

Rees, D., & Fuller-Rowell, T. J. (1992). Modelling the response of the thermosphere/ionosphere system to time dependent forcing. *Advances in Space Research*, *12*(6), 69–87. https://doi.org/10.1016/0273-1177(92)90041-U

Reinisch, B. W., Galkin, I. A., Khmyrov, G. M., Kozlov, A. V., Bibl, K., Lisysyan, I. A., Cheney, G. P., Huang, X., Kitrosser, D. F., Paznukhov, V. V., Luo, Y., Jones, W., Stelmash, S., Hamel, R., & Grochmal, J. (2009). New Digisonde for research and monitoring applications. *Radio Science*, *44*(1), RS0A24. https://doi.org/10.1029/2008RS004115

Reinisch, B. W., & Galkin, I. A. (2011). Global ionospheric radio observatory (GIRO). *Earth, Planets and Space*, *63*, 377–381. https://doi.org/10.5047/eps.2011.03.001

Richards, P. G., Schunk, R. W., & Sojka, J. J. (1983). Large-scale counterstreaming of H^+ and He^+ along plasmaspheric flux tubes. *Journal of Geophysical Research*, *88*(A10), 7879–7886. https://doi.org/10.1029/JA088iA10p07879

Richards, P. G., Buonsanto, M. J., Reinisch, B. W., Holt, J., Fennelly, J. A., Scali, J. L., Comfort, R. H., Germany, G. A., Spann, J., Brittnacher, M., & Fok, M.-C. (2000). On the relative importance of convection and temperature to the behavior of the ionosphere in North America during January 6–12, 1997. *Journal of Geophysical Research: Space Physics*, *105*(A6), 12763–12776. https://doi.org/10.1029/1999JA000253

Rishbeth, H. (1998). How the thermospheric circulation affects the ionospheric F2-layer. *Journal of Atmospheric and Solar-Terrestrial Physics*, *60*(14), 1385–1402. https://doi.org/10.1016/S1364-6826(98)00062-5

Rush, C., Fox, M., Bilitza, D., Davies, K., McNamara, L., Stewart, F., & Pokempner, M. (1989). Ionospheric mapping – an update of foF2 coefficients. *Telecommunication Journal*, *56*(3), 179–182.

Shinbori, A., Otsuka, Y., Sori, T., Tsugawa, T., & Nishioka, M. (2022). Statistical behavior of large-scale ionospheric disturbances from high latitudes to mid-latitudes during geomagnetic storms using 20-yr GNSS-TEC data: Dependence on season and storm intensity. *Journal of Geophysical Research: Space Physics*, *127*(1), e2021JA029687. https://doi.org/10.1029/2021JA029687

Shubin, V. N. (2015). Global median model of the F2-layer peak height based on ionospheric radio-occultation and ground-based Digisonde observations. *Advances in Space Research*, *56*(5), 916–928. https://doi.org/10.1016/j.asr.2015.05.029

Shulha, M. O., Kotov, D. V., Bogomaz, O. V., Zhivolup, T. G., Koloskov, O. V., Lisachenko, V. M., & Hairston, M. (2019). Multi-instrumental and modeling investigation of ionospheric response to weak geomagnetic storm of 21–23 March 2017 over the Ukrainian Antarctic station and magnetically conjugate region. In *Book of Abstracts "IX International Antarctic Conference dedicated to the 60th anniversary of the signing of the Antarctic Treaty in the name of peace and development of international cooperation"* (pp. 185–186). SI NASC. http://uac.gov.ua/international-cooperation/mak/mak-2019/

Zalizovski, A. V., Kashcheiev, A. S., Kashcheiev, S. B., Koloskov, A. V. , Lisachenko, V. N., Paznukhov, V. V., Pikulik, I. I., Sopin, A. A., & Yampolski, Yu. M. (2018). A prototype of a portable coherent ionosonde. *Space Science and Technology*, *24*(3), 10–22. https://doi.org/10.15407/knit2018.03.010

Received: 21 February 2022
Accepted: 18 June 2022

М. Резниченко[1, *], О. Богомаз[1, 2], Д. Котов[1], Т. Живолуп[1], О. Колосков[3, 2], В. Лисаченко[3]

[1] Інститут іоносфери НАН України, МОН України, м. Харків, 61001, Україна
[2] Державна установа Національний антарктичний науковий центр МОН України, м. Київ, 01601, Україна
[3] Радіоастрономічний інститут НАН України, м. Харків, 61002, Україна

*** Автор для кореспонденції:** marina.shulga23@gmail.com

Спостереження іоносфери за допомогою іонозондів у Південній та Північній півкулях під час подій у геокосмосі в жовтні 2021 року

Реферат. У статті представлено результати спостережень іоносфери над Українською антарктичною станцією «Академік Вернадський» та обсерваторією Міллстоун Хілл (США). Розглянуто варіації таких параметрів іоносфери як висота та електронна концентрація максимуму області F2 іоносфери (h_{mF2} та N_{mF2}) у жовтні 2021-го року. Наведено результати порівняльного аналізу результатів спостережень та прогнозів моделі іоносфери International Reference Ionosphere 2016 (IRI-2016). Метою роботи є дослідження реакції іоносфери на вплив космічної погоди в Північній та Південній півкулях американського довготного сектору за допомогою іонозондів, розміщених на станції «Академік Вернадський» і поблизу магнітоспряженого регіону (Міллстоун Хілл) та порівняння результатів спостережень з модельними значеннями. Висота області F2 іоносфери розраховувалася шляхом реконструкції висотних профілів концентрації електронів з іонограм, які отримано за допомогою іонозондів. Для порівняння з результатами спостережень використовувалися добові варіації h_{mF2} та N_{mF2}, які були розраховані за допомогою низки субмоделей моделі IRI-2016. Виявлено сильну негативну реакцію іоносфери на помірне геомагнітне збурення 12 жовтня як над станцією «Академік Вернадський», так і над Міллстоун Хілл. Спостерігалося поступове нічне збільшення концентрації електронів (приблизно удвічі) протягом 21–31 жовтня над станцією. Виявлено, що субмоделі висоти максимуму області F2 іоносфери (SHU-2015 та AMTB-2013) в цілому добре описують отримані експериментальним шляхом варіації h_{mF2} як у денні, так і в нічні години протягом майже всього досліджуваного періоду як над станцією «Академік Вернадський», так і над Міллстоун Хілл. Найбільші відхилення для обох субмоделей спостерігаються в нічні години магнітозбурених періо-

дів. Субмоделі концентрації електронів (URSI та CCIR) здебільшого добре відтворюють спостережувані варіації $N_{m\mathrm{F2}}$. У той же час, спостерігаються відмінності між результатами спостережень та прогнозами моделей під час магнітозбурених умов. За результатами розрахунків середнього квадратичного відхилення не можна зробити висновок, що якась з субмоделей IRI-2016 є кращою у порівнянні з іншими. Наведено та обговорено гіпотези щодо ймовірних причин відмінностей у експериментальних та модельних варіаціях $h_{m\mathrm{F2}}$ та $N_{m\mathrm{F2}}$ в рамках відомих механізмів іоносферних бур. Результати, отримані в даній роботі, демонструють особливості стану іоносфери в різних півкулях американського довготного сектору в магнітоспокійних і збурених умовах та є ще однією перевіркою сучасних емпіричних міжнародних довідкових моделей іоносфери.

Ключові слова: вертикальне зондування іоносфери, висота максимуму шару F2, геокосмічна буря, концентрація електронів, модель іоносфери